



Tuning the anticancer activity of maltol-derived ruthenium complexes by derivatization of the 3-hydroxy-4-pyrone moiety

Wolfgang Kandioller^a, Christian G. Hartinger^{a,b,*}, Alexey A. Nazarov^{a,b,*}, Johanna Kasser^a, Roland John^a, Michael A. Jakupec^a, Vladimir B. Arion^a, Paul J. Dyson^b, Bernhard K. Keppler^a

^aUniversity of Vienna, Institute of Inorganic Chemistry, Waehringer Str. 42, A-1090 Vienna, Austria

^bInstitut des Sciences et Ingénierie Chimiques, Ecole Polytechnique Fédérale de Lausanne (EPFL), CH-1015 Lausanne, Switzerland

ARTICLE INFO

Article history:

Received 12 September 2008

Received in revised form 9 October 2008

Accepted 10 October 2008

Available online 17 October 2008

Dedicated to Prof. Gérard Jaouen on the occasion of his 65th birthday.

Keywords:

Antitumor agents

Bioorganometallic chemistry

Ruthenium(II)-arene complex

Pyrone

Hydrolysis

5'-GMP binding

ABSTRACT

Organometallic ruthenium(II)-arene complexes coordinated to maltol-derived ligands were prepared and their anticancer activity against human tumor cell lines was studied. In addition, their hydrolysis behavior and reaction with 5'-GMP was tested and compared to the parent compound chlorido[2-methyl-3-(oxo-κO)-pyran-4(1H)-onato-κO4](η⁶-p-cymene)ruthenium(II) (Ru-maltol). Improved stability and *in vitro* anticancer activity at maintained GMP binding capability were observed, in comparison to the Ru-maltol complex.

© 2008 Elsevier B.V. All rights reserved.

1. Introduction

Platinum complexes play an important role in the treatment of cancer and are included into *ca.* 50% of the therapeutic schemes [1]. Due to severe side effects, high toxicity, limited activity in common tumor types and tumor resistance, non-platinum complexes are undergoing intensive research as chemotherapeutics and also as radiodiagnostics [2–7]. Ruthenium compounds are the most widely developed alternatives, and (H₂Ind) *trans*-[RuCl₄(HInd)₂] (KP1019, HInd = indazole; Fig. 1) and (H₂Im) *trans*-[RuCl₄(DMSO)-(HIm)] (NAMI-A, HIm = imidazole) have entered clinical trials [4,8,9]. Both compounds exhibit only low side effects, which might be due to selective uptake *via* the transferrin cycle [10–15] and/or activation by reduction [16] in the reductive environment typical of neoplastic tissue.

More recently stable organometallic compounds moved into the focus of interest [5]. Beside, for example, titanium, iron and

* Corresponding authors. Address: University of Vienna, Institute of Inorganic Chemistry, Waehringer Str. 42, A-1090 Vienna, Austria. Tel.: +43 1 4277 52609; fax: +43 1 4277 52680 (C.G. Hartinger).

E-mail addresses: christian.hartinger@univie.ac.at (C.G. Hartinger), alex.nazarov@univie.ac.at (A.A. Nazarov).

gold compounds [17–19], some of which underwent clinical trials, Ru(II) species, such as RAPTA type complexes, have been observed to exhibit anticancer activity, tunable by careful selection of the ligand sphere [3,20–32]. These studies resulted in compounds with interesting modes of action, for example potentially targeting kinases [25,29,30], or drug resistance pathways [27,33] and light activated systems [34,35], and a number of encouraging *in vivo* studies have been reported [3,5,21,22,36,37]. More recently, dinuclear pyridinone-based Ru(II) complexes, such as PyrRu₂¹² (Fig. 1), were observed to exhibit increased cytotoxicity due to jointly acting Ru(II)-arene moieties [31,32,38]. By varying the spacer length between the two ruthenium centers, compounds with mild to high cytotoxicity were obtained. Recent studies on their DNA binding properties revealed different modes of action for compounds only varying in the length of the spacer between the Ru(II)-arene fragments [31,32,38]. Other maltol-derived compounds have proven medicinal potential in the treatment of β-thalassemia and diabetes, and as radiodiagnostics [39] and, when coordinated to a Ga(III) center, in chemotherapy [2], or in form of a VO(maltolato) complex as a medication against diabetes type II [40,41].

The coordination ability of maltol-derived ligands with particular affinities for divalent and trivalent metal ions allows very stable complexes to be prepared [31,32,42–45], which can easily be

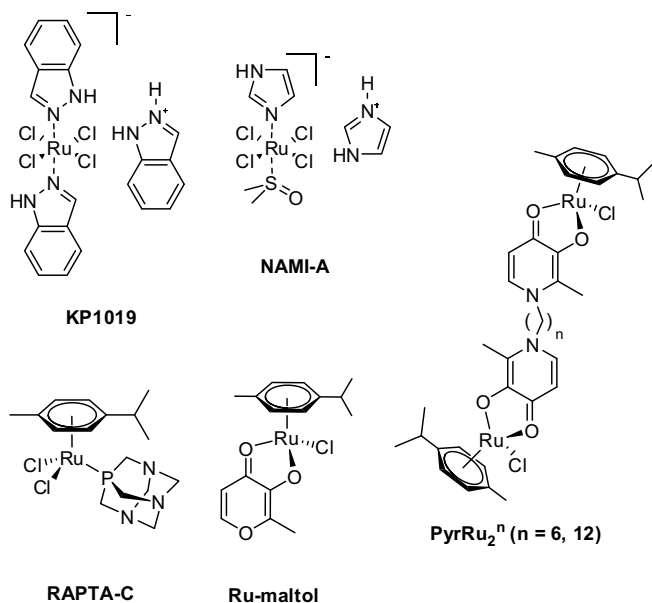


Fig. 1. Structural formulae of the ruthenium anticancer drug candidates KP1019, NAMI-A, RAPTA-C, Ru-maltol and PyrRu_2^n .

varied for modulation of important parameters such as solubility, hydrophobicity, etc.

In the present work, the synthesis of mononuclear Ru(II)-arene complexes with novel maltol-derived ligands is reported. The substitution pattern of the aryl part of the ligand was found to be crucial for controlling both the *in vitro* anticancer activity and complex solubility.

2. Results and discussion

2.1. Synthesis and characterization of the Ru(II)-*p*-cymene complexes

The synthesis of the precursor allomaltol **1** was performed in two steps, starting from kojic acid by reaction with thionylchloride followed by the reduction with zinc under acidic conditions (Scheme 1) [46]. Due to the higher reactivity of position 2 compared to 5 in the pyrone ring of **1**, functionalization can easily be

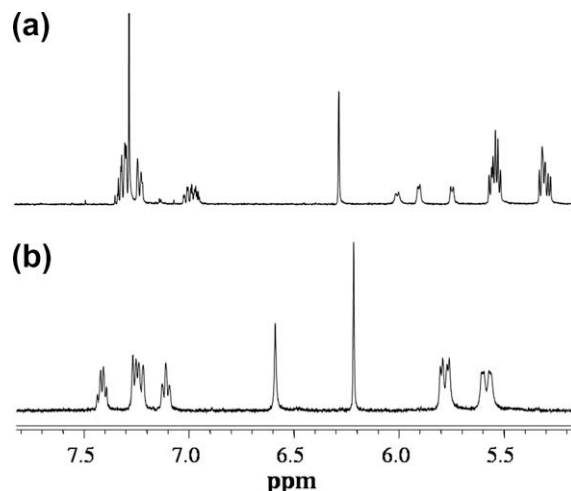
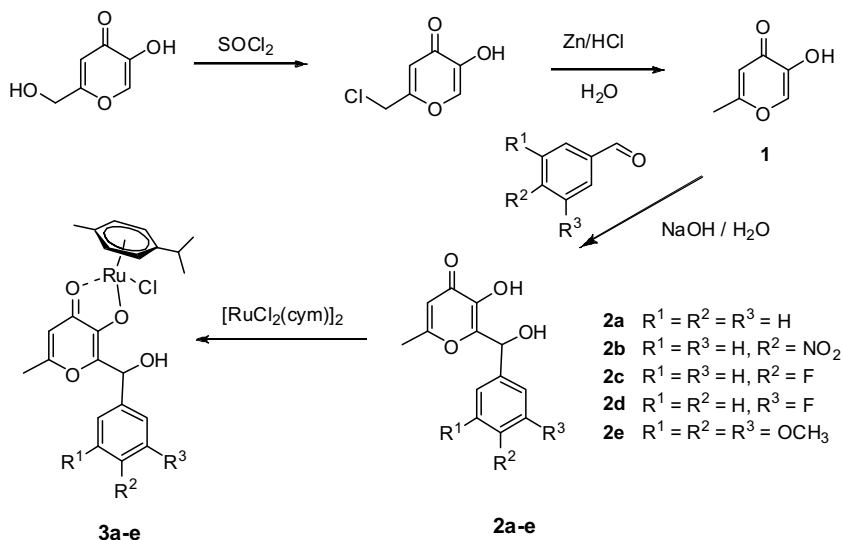


Fig. 2. $^1\text{H NMR}$ of **3d** in (a) CDCl_3 and (b) D_2O .

achieved in a similar fashion to the aldol reaction. Compound **1** was deprotonated with NaOH, and the anionic species obtained was reacted immediately with the corresponding aldehyde, yielding ligands **2a–e** after addition of HCl and recrystallization (yield 64–90%). The reaction occurs only in sufficient yield at pH 10.5. The air and light stable complexes (>1 year) **3a–e** were obtained by deprotonation of the corresponding ligand with sodium methoxide and addition of the bis[dichlorido(η^6 -*p*-cymene)ruthenium(II)]. A slight excess of ligand (10%) was added in order to facilitate purification, and all complexes were obtained in good yield (52–73%).

The compounds were characterized by IR and 1D and 2D NMR spectroscopy, mass spectrometry and elemental analysis. All complexes possess two stereogenic centers and were isolated as mixtures of two diastereomers (*R/R*, *S/S* and *R/S*, *S/R*), as observed by NMR spectroscopy in aprotic solvents, where both forms are distinguishable. The separation of the diastereomers by fractional crystallization or chromatography was not successful. As a representative example, the $^1\text{H NMR}$ of **3d** in CDCl_3 and in D_2O is shown in Fig. 2. In CDCl_3 two sets of signals are observed for the hydrogens of the coordinated arene ring and for the *m*-fluoro substituted phenyl group. In D_2O , the spectrum comprises a single



Scheme 1. Synthesis of pyrone-based ligands and their ruthenium(II)-arene complexes.

set of signals, presumably due to fast inversion of the metal center, leading to epimerization of the diastereomers [47,48]. The ^1H NMR signal of the OH proton was observed to be split in aprotic solvents into two doublets with $\Delta\delta = 0.2$ ppm, which may be due to the formation of a hydrogen bond between the aliphatic –OH group of the ligand and the coordinated alcoholate of the pyrone ring (Fig. 2).

The IR spectra of the ligands **2a–e** show C=O, C=C and C–O stretching bands at 1654–1120 cm^{-1} [49]. The O–H stretching bands were observed as broad bands in the range 3420–3280 cm^{-1} . The spectra of **3a–d** contained four bands in the region of 1610–1460 cm^{-1} , which are typical for maltolato complexes [50,51]. Upon complexation the C=O stretching bands appear shifted by 40 cm^{-1} to lower wavenumbers. In the case of **3e** strong overlapping of the latter signals with those assignable to the methoxy groups was observed. In the spectra of the complexes the bands attributed to the OH stretching are in the range 3400–3340 cm^{-1} and are of significantly lower intensity due to deprotonation and coordination of one of the OH groups to the Ru centers.

ESI mass spectra of **3a–e** were recorded in methanol in the positive ion mode. For all compounds the most abundant peaks were assigned to $[\text{M}–\text{Cl}]^+$ ions, which had the appropriate ruthenium isotopic pattern.

2.2. Crystal structure determination

The molecular structure of **3b** was determined by X-ray diffraction analysis (Fig. 3), and the metal center was found to adopt the expected pseudo-octahedral “piano-stool” geometry. In the phenyl substituted maltolato complex **3b** and PyrRu_2^6 a short and a long Ru–O bond have been observed (Table 1), whereas in chlorido-[3-(oxo- κO)-2-methyl-4-pyridinonato- κO4](η^6 -*p*-cymene)ruthenium(II) (Ru-maltol, Fig. 1) the two Ru–O bond lengths are almost identical. This observation might be explained by a lengthening of the Ru–O2 bond in the Ru-maltol complex due to the involvement of this oxygen donor atom in a strong intermolecular H-bond (donor–acceptor distance of 2.805(2) Å, and a donor–hydrogen–acceptor angle of 174°). The Ru–Cl bond length in **3b** of 2.4310(4) Å is similar to that in Ru-maltol, whereas the bond observed for the pyridinone complex PyrRu_2^6 is slightly shorter [31]. Although the Ru–Cl bond lengths in the above mentioned structures are very different, the rate of hydrolysis is rapid in all cases (see below).

2.3. Hydrolysis, pK_a and GMP binding

Due to the low solubility of **3a–e** in water (Table 2), all NMR experiments on the hydrolytic stability were performed in a 5%

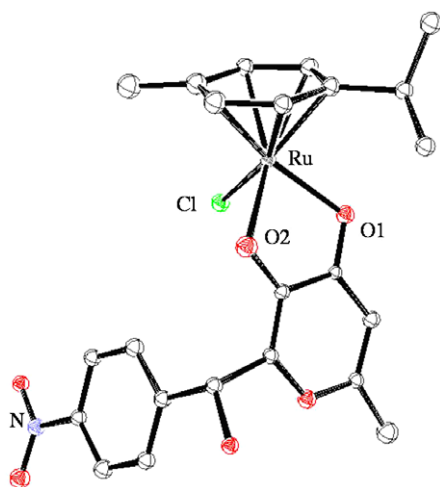


Fig. 3. ORTEP plot of the molecular structure of **3b** at 50% probability level.

Table 1

Selected bond lengths (Å) and angles ($^\circ$) of **3b** and comparisons with the dinuclear complex PyrRu_2^6 and the structurally related Ru-maltol complex chlorido[3-(oxo- κO)-2-methyl-4-pyridonato- κO4](η^6 -*p*-cymene)ruthenium(II).

| | 3b | PyrRu_2^6 ^a | Ru-maltol ^b |
|----------|------------|---------------------------------|------------------------|
| Ru–Cl | 2.4310(4) | 2.4186(10) | 2.4329(5) |
| Ru–O1 | 2.1179(10) | 2.101(3) | 2.1035(13) |
| Ru–O2 | 2.0766(10) | 2.074(3) | 2.0901(13) |
| O1–Ru–O2 | 78.82(4) | 79.63(11) | 78.79(5) |
| O1–Ru–Cl | 83.35(3) | 83.90(8) | 83.42(4) |
| Cl–Ru–O2 | 85.51(3) | 85.11(8) | 85.89(4) |

^a From Ref. [31].

^b From Ref. [28].

Table 2

Solubility in PBS and IC_{50} values of **3a–e** and of Ru-maltol in the human cancer cell lines CH1, SW480 and A549.

| Compound | Solubility (mg/mL) | IC_{50} (μM) | | |
|-----------|--------------------|------------------------------------|-------------|--------------|
| | | CH1 | SW480 | A549 |
| 3a | 0.25 | 50 \pm 9 | 67 \pm 10 | 172 \pm 5 |
| 3b | Insoluble | – | – | – |
| 3c | 0.1 | 24 \pm 4 | 44 \pm 10 | 98 \pm 4 |
| 3d | 0.1 | 29 \pm 2 | 57 \pm 8 | 138 \pm 6 |
| 3e | 1 | 48 \pm 6 | 84 \pm 7 | 220 \pm 14 |
| Ru-maltol | >10 | >100 | >100 | – |

DMSO- d_6 /D $_2$ O solution. Coordination of DMSO to the ruthenium center was not observed (data not shown). NMR spectra of the complexes with and without addition of AgNO_3 (used to remove the chlorido ligand) are identical, indicating that the hydrolysis proceeds immediately upon dissolving in water. The aqua complexes are stable in aqueous solution, whereas the Ru-maltol complex reacts to form a dimeric ruthenium compound [28], indicating that the hydroxyl-methyl-aryl substituent in position 2 of the pyrone ring inhibits the formation of dimeric species.

The pK_a values of the aqua complexes of **3a–e** were estimated by titration with NaOD to afford the corresponding hydroxido compounds by monitoring the deprotonation process by ^1H NMR spectroscopy (Table 3). To generate the aqua species, the complexes were dissolved in D $_2$ O containing 5% DMSO- d_6 . The chemical shifts of the $\text{Ar}_{\text{cym}}\text{-H2/H6}$ proton signal of the arene ring (e.g., from 5.75 ppm at pH 3.21 to 5.49 at pH 11.00 for **3c**) were plotted against the pD value. The pK_a values (in D $_2$ O) were determined from the inflection point of the sigmoid curve (see Fig. 4 for the titration curve of **3c**) and corrected for the difference between D $_2$ O and water to yield the pK_a (using Eq. (1), see Section 4). The pK_a values of **3a–e** were determined to be between 8.99 and 9.80, with the substitution of the aryl moiety of the ligand having only a minor influence. The pK_a values are similar to those of the parent compound Ru-maltol (pK_a 9.23) [28] and the dinuclear pyridinone-type ruthenium arene complexes (pK_a 9.60–9.83) [31].

The reaction of **3a–e** with the DNA model compound 5'-GMP was investigated by ^1H and ^{31}P NMR spectroscopy to evaluate the potential of DNA as an intracellular target, as reported for other Ru complexes and also the clinically established Pt compounds

Table 3

pK_a values of complexes **3a–e**.

| Compound | pK_a |
|-----------|-----------------|
| 3a | 9.05 \pm 0.02 |
| 3b | 9.80 \pm 0.03 |
| 3c | 8.99 \pm 0.01 |
| 3d | 9.56 \pm 0.01 |
| 3e | 9.64 \pm 0.02 |

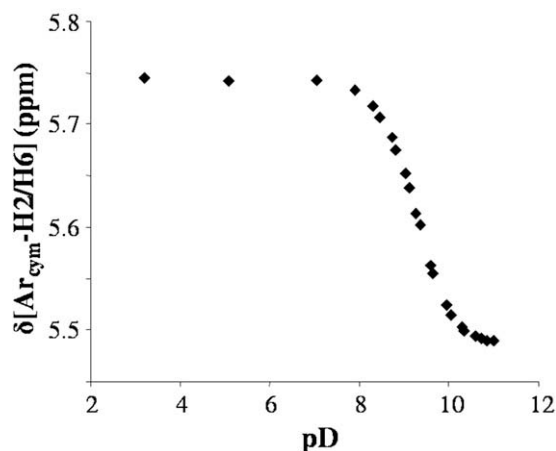


Fig. 4. Titration curve of **3c** used to determine the pK_a .

[1,16,52,53]. Stepwise addition of 5'-GMP to the aqua complexes (in aqueous solutions) resulted in the formation of 5'-GMP adducts within seconds. After addition of an equimolar amount of the reagent, three new signals for the H8 of 5'-GMP were observed in the ^1H NMR spectra between 7.7 and 7.9 ppm in a ratio of 1:1:2 (Fig. 5). The signals may be assigned to the four stereoisomers formed by the coordination of 5'-GMP to the ruthenium center. The change of the H8 signal in the ^1H NMR spectrum from 8.15 ppm to approximately 7.80 ppm indicates coordination *via* the N7 atom of the guanine [53]. The ^{31}P NMR spectrum contains 3 peaks between 3.7 and 3.1 ppm in 1:1:2 ratio in agreement with the ^1H NMR spectra.

2.4. *In vitro* evaluation

The *in vitro* anticancer activity of **3a** and **3c–e** was determined in SW480 (colon carcinoma), CH1 (ovarian carcinoma) and A549 (non-small cell lung carcinoma) human cancer cells using the colorimetric MTT assay, yielding IC_{50} values mostly in the 10^{-5} M range (Table 2). Due to the low solubility of **3b** it was not possible to determine its anticancer activity.

CH1 cells were found to be the most sensitive to all four ruthenium complexes, and in all cell lines **3c** was the most active compound with an IC_{50} value of 24 μM in the ovarian cancer cell line (Fig. 6). In general, it appears as the solubility in medium/DMSO

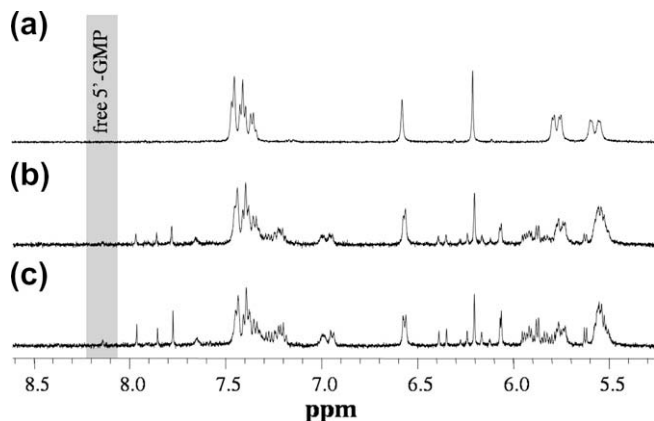


Fig. 5. 5'-GMP binding of **3d** studied by ^1H NMR spectroscopy after addition of (a) 0 eq, (b) 1 eq, and (c) an excess of 5'-GMP to a D_2O solution of the Ru complex.

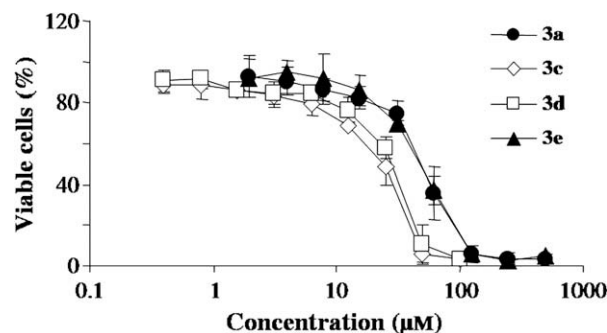


Fig. 6. Concentration–effect curves of **3a** and **3c–e** in CH1 ovarian carcinoma cells.

as a measure of lipophilicity determines the *in vitro* anticancer activity of the compounds (Table 2). Furthermore, the substituent on the aryl moiety of the ligand appears to influence the activity of the ruthenium complex in all tested cell lines: **3c** and **3d** with their electron withdrawing substituents exhibit a higher cytotoxic activity in CH1 cells than **3a**. In contrast, electron-donating substituents such as the methoxy groups in **3e** do not significantly influence the activity in CH1 cells and are even disadvantageous in SW480 and A549 cells. In comparison to the parent compound Ru-maltol, the compounds bearing substituents at the 2-position are more cytotoxic, which may also be due to the increased lipophilicity of the compounds (Table 2). However, in order to establish definitive structure–activity relationships a higher number of compounds need to be studied.

3. Conclusions

Ruthenium complexes have been established as potential drug candidates for treatment of cancer. Herein, ruthenium(II)-*p*-cymene complexes with 2-substituted 3-hydroxypyran-4(1*H*)-one ligands have been evaluated for potential anticancer activity. The complexes hydrolyze rapidly in aqueous solutions, in a process involving substitution of the chlorido ligand by an aqua ligand. Substitution of the 2-position of the pyrone moiety results in increased stability of the aqua complexes in aqueous solution in comparison to Ru-maltol which affords dimeric species. The reaction of the Ru moiety toward 5'-GMP is very fast, and binding occurs selectively at the N7 of the guanine. Complexes **3a** and **3c–e** exhibit moderate cytotoxicity against SW480 and CH1 human tumor cell lines, and poor activity against A549 cells, suggesting a certain degree of selectivity. The aryl moiety seems to be relevant for determining the *in vitro* activity of the compounds with electron withdrawing substituents at the phenyl moiety decreasing the IC_{50} value and electron donating groups having the opposite effect. There appears to be a correlation between the electronic effect of the substituents on the maltol-derived ligands, and the *in vitro* activity, but a larger library of compounds should be studied to confirm this hypothesis.

4. Experimental

4.1. Materials and methods

All solvents were dried and distilled prior to use. Ruthenium(III) chloride (Johnson Matthey), kojic acid (Fluka), benzaldehyde (Fluka), *p*-nitrobenzaldehyde (Aldrich), *p*-fluorobenzaldehyde (Fluka), *m*-fluorobenzaldehyde (Fluka), 3,4,5-trimethoxybenzaldehyde (Aldrich) and sodium methoxide (Aldrich) were purchased and used without further purification. Bis[dichlorido(η^6 -*p*-cymene)ruthenium(II)], 2-chloromethyl-5-hydroxypyran-4(1*H*)-one (chlorokojic acid), and 5-hydroxy-2-methyl-pyran-4(1*H*)-one

(allomaltol, **1**) were synthesized as described elsewhere [46,54]. Melting points were determined with a Büchi B-540 apparatus and are uncorrected. Elemental analyses were carried out with a Perkin Elmer 2400 CHN Elemental Analyzer at the Microanalytical Laboratory of the University of Vienna. NMR spectra were recorded at 25 °C on a Bruker FT-NMR spectrometer Avance IIITM 500 MHz at 500.10 MHz (¹H), 125.75 MHz (¹³C) and 202.44 MHz (³¹P) in DMSO-*d*₆, D₂O or CDCl₃. The 2D NMR spectra were measured in a gradient-enhanced mode. An esquire₃₀₀₀ ion trap mass spectrometer (Bruker Daltonics, Bremen, Germany), equipped with an orthogonal ESI ion source, was used for MS measurements. The solutions were introduced via flow injection using a Cole-Parmer 74900 single-syringe infusion pump (Vernon Hills, IL). The ESI-MS instrument was controlled by means of the ESQUIRECONTROL software (version 5.2), and all data were processed using DATAANALYSIS software (version 3.2) (both Bruker Daltonics). IR spectra were measured in KBr matrix (4000–400 cm⁻¹) with a Bruker Vertex 70 FT-IR spectrometer.

Single crystals of **3b** were grown from MeOH, and X-ray diffraction measurement was performed on a Bruker X8 APEXII CCD diffractometer at 100 K. The single crystal was positioned at 40 mm from the detector, and 2965 frames were measured, each for 3 s over 1° scan width. The data were processed using the SAINT software package [55]. Crystal data, data collection parameters, and structure refinement details are given in Table 4. The structure was solved by direct methods and refined by full-matrix least-squares techniques. Non-hydrogen atoms were refined with anisotropic displacement parameters. H atoms were inserted at calculated positions and refined with a riding model. The following computer programs were used: structure solution, SHELXS-97 [56]; refinement, SHELXL-97 [57]; molecular diagrams, ORTEP-3 [58]; computer, Pentium IV; scattering factors [59].

Table 4
Crystal data and details of data collection for **3b**.

| | |
|---|--|
| Chemical formula | C ₂₃ H ₂₄ ClNO ₆ Ru |
| <i>M</i> (g mol ⁻¹) | 546.95 |
| Temperature (K) | 100(2) |
| Crystal size (mm) | 0.30 × 0.30 × 0.20 |
| Crystal color, shape | Orange, block |
| Crystal system | Triclinic |
| Space group | <i>P</i> $\bar{1}$ (No 2) |
| <i>a</i> (Å) | 7.4276(4) |
| <i>b</i> (Å) | 12.5755(5) |
| <i>c</i> (Å) | 12.6091(6) |
| α (°) | 72.009(2) |
| β (°) | 87.811(3) |
| γ (°) | 74.210(2) |
| <i>V</i> (Å ³) | 1076.55(9) |
| <i>Z</i> | 2 |
| <i>D</i> _c (g cm ⁻³) | 1.687 |
| μ (cm ⁻¹) | 8.94 |
| <i>F</i> (000) | 556 |
| θ Range for data collection (°) | 2.04–30.07 |
| <i>h</i> range | –10/10 |
| <i>k</i> range | –17/17 |
| <i>l</i> range | –17/17 |
| Number of reflections used in refinement | 6280 |
| Number of parameters | 295 |
| <i>R</i> _{int} | 0.0354 |
| <i>R</i> ₁ ^a | 0.0212 |
| <i>wR</i> ₂ ^b | 0.0532 |
| GOF ^c | 1.007 |
| Residuals (e ⁻ Å ⁻³) | 0.592, –0.490 |

^a $R_1 = \sum ||F_o| - |F_c|| / \sum |F_o|$.

^b $wR_2 = \{ \sum [w(F_o^2 - F_c^2)^2] / \sum w(F_o^2)^2 \}^{1/2}$.

^c GOF = $(\sum [w(F_o^2 - F_c^2)^2] / (n - p))^{1/2}$, where *n* is the number of reflections and *p* is the total number of parameters refined.

4.2. Synthesis

4.2.1. General procedure for the reaction of allomaltol with the aldehydes

Allomaltol **1** (1 eq) and NaOH (1.1 eq) were dissolved in water and stirred for 5 min. Afterwards, the aldehyde (1.1 eq) was added dropwise to the reaction mixture. The solution was adjusted to pH 10.5 with 5 M NaOH solution and stirred at r.t. for 12 h. The reaction mixture was acidified to pH 1 with conc. HCl and the resulting precipitate was collected by filtration. If no precipitation occurred, the reaction mixture was extracted with CH₂Cl₂ (3 × 20 mL). The combined organic layers were washed twice with saturated NaHCO₃ (30 mL) and water (30 mL), dried over Na₂SO₄, filtered and concentrated *in vacuo*. The crude product was purified by recrystallization.

4.2.1.1. 2-(Hydroxy-phenyl-methyl)-3-hydroxy-6-methyl-pyran-4(1H)-one (2a). The reaction was performed according to the general procedure using **1** (2.0 g, 15.8 mmol) and benzaldehyde (1.8 mL, 17.5 mmol). The crude product was recrystallized from 2-propanol affording a white powder (3.3 g, 90%). M.p. 170–172 °C (decomp.); ¹H NMR (DMSO-*d*₆) δ : 2.18 (s, 3H, CH₃), 5.99 (d, *J* = 4.5 Hz, 1H, CHOHP), 6.14 (d, *J* = 5.0 Hz, 1H, CHOHP), 6.19 (s, 1H, CH), 7.27 (t, *J* = 7.5 Hz, 1H, Ph-H4'), 7.35 (t, *J* = 7.5 Hz, 2H, Ph-H3'/H5'), 7.40 (d, *J* = 7.5 Hz, 2H, Ph-H2'/H6'); ¹³C NMR (DMSO-*d*₆) δ : 19.7 (CH₃), 66.3 (CHPhOH), 111.6 (CH₃C=CH), 126.4 (Ph-C2'), 127.8 (Ph-C4'), 128.7 (Ph-C3') 141.0 (CH₃C=CH), 141.8 (Ph-C1'), 151.0 (HOCHC=COH), 165.0 (CHOH), 174.3 (C=O); IR (KBr, cm⁻¹, selected bands): 3323, 1654, 1607, 1562, 1256, 1209; Elemental Anal. Calc. for C₁₃H₁₂O₄ · 0.2H₂O: C, 66.20; H, 5.30. Found: C, 66.24; H, 5.33%.

4.2.1.2. 2-[(4-Nitrophenyl)-hydroxy-methyl]-3-hydroxy-6-methyl-pyran-4(1H)-one (2b). The reaction was performed according to the general procedure using **1** (1.00 g, 7.9 mmol) and 4-nitrobenzaldehyde (1.32 g, 8.7 mmol, in 2 mL dioxane). The crude product was purified by recrystallization from 2-propanol affording yellow crystals (1.41 g, 64%). M.p. >200 °C decomp.; ¹H NMR (DMSO-*d*₆) δ : 2.17 (s, 3H, CH₃), 6.13 (s, 1H, CHOAr), 6.21 (s, 1H, CH), 6.50 (brs, 1H, CHOAr), 7.66 (d, *J* = 8.8 Hz, 2H, Ar-H2'/H6'), 8.23 (d, *J* = 8.6 Hz, 2H, Ar-H3'/H5'), 9.34 (s, 1H, COH); ¹³C NMR (DMSO-*d*₆) δ : 20.1 (CH₃), 66.2 (CHOAr), 112.1 (CH₃C=CH), 124.4 (Ar-C2'/C6'), 128.0 (Ar-C3'/C5'), 141.9 (CH₃C=CH), 147.7 (Ar-C1'), 149.8 (Ar-C4'), 150.2 (HOCHC=COH), 165.6 (CHOH), 174.7 (C=O); IR (KBr, cm⁻¹, selected bands): 3281, 1650, 1606, 1563, 1347, 1220; Elemental Anal. Calc. for C₁₃H₁₁NO₆ · 0.1H₂O: C, 55.95; H, 4.04; N, 5.01. Found: C, 55.90; H, 3.98; N, 4.98%.

4.2.1.3. 2-[(4-Fluorophenyl)-hydroxy-methyl]-3-hydroxy-6-methyl-pyran-4(1H)-one (2c). The reaction was performed according to the general procedure using **1** (1.00 g, 8.0 mmol) and 4-fluorobenzaldehyde (1.08 g, 8.8 mmol, in 1 mL dioxane), affording colorless crystals (1.80 g, 91%). M.p. 158–160 °C; MS (ESI⁻) *m/z* 249 [M–H]⁻; ¹H NMR (DMSO-*d*₆) δ : 2.19 (s, 3H, CH₃), 5.99 (s, 1H, CHOAr), 6.20 (s, 1H, CH), 6.19 (brs, 1H, CHOAr), 7.18 (t, *J* = 9.0 Hz, 2H, Ar-H3'/H5'), 7.43 (dd, *J* = 9.0 Hz, *J* = 3.0 Hz, Ar-H2'/H6'), 9.10 (brs, 1H, COH); ¹³C NMR (DMSO-*d*₆) δ : 19.7 (CH₃), 66.7 (CHOAr), 111.6 (CH₃C=CH), 115.5 (*J* = 21.5 Hz, Ar-C3'), 128.4 (*J* = 8.1 Hz, Ar-C2'), 138.0 (*J* = 3.0 Hz, Ar-C1'), 141.0 (CH₃C=CH), 150.7 (HOCHC=COH), 161.9 (*J* = 242.0 Hz, Ar-C4'), 165.1 (CHOH), 174.3 (C=O); IR (KBr, cm⁻¹, selected bands): 3293, 1652, 1607, 1564, 1508, 1219; Elemental Anal. Calc. for C₁₃H₁₁FO₄ · ¼H₂O: C, 61.30; H, 4.55. Found: C, 61.56; H, 4.39%.

4.2.1.4. 2-[(3-Fluorophenyl)-hydroxy-methyl]-3-hydroxy-6-methyl-pyran-4(1H)-one (2d). The reaction was performed according to

the general procedure using **1** (0.50 g, 4.0 mmol) and 3-fluorobenzaldehyde (0.54 g, 4.4 mmol, in 1 mL dioxane) affording colorless crystals (0.85 g, 85%). M.p. 170–172 °C; ¹H NMR (DMSO-*d*₆) δ: 2.27 (s, 3H, CH₃), 6.01 (s, 1H, CHOAr), 6.20 (s, 1H, CH), 6.40 (brs, CHOAr) 7.10 (m, Ar-H4'), 7.18–7.21 (m, 2H, Ar-H2'/H6'), 7.38 (q, *J* = 8.0 Hz, Ar-H5'), 9.15 (brs, 1H, COH); ¹³C NMR (DMSO-*d*₆) δ: 19.7 (CH₃), 66.8 (CHOAr), 111.7 (CH₃C=CH) 113.0 (*J* = 22.1 Hz, Ar-C2'), 114.6 (*J* = 21.3 Hz, Ar-C4'), 122.4 (*J* = 3.0 Hz, Ar-C6'), 130.7 (*J* = 8.2 Hz, Ar-C5') 141.2 (CH₃C=CH), 144.8 (*J* = 8.3 Hz, Ar-C1'), 150.4 (HOCHC=COH), 162.0 (*J* = 242.1 Hz, Ar-C3'); 165.1 (CHOH), 174.3 (C=O); IR (KBr, cm⁻¹, selected bands): 3293, 1655, 1609, 1561, 1252, 1208; Elemental Anal. Calc. for C₁₃H₁₁FO₄ · ¼H₂O: C, 61.30; H, 4.55. Found: C, 61.30; H, 4.45%.

4.2.1.5. 2-[(3,4,5-Trimethoxyphenyl)-hydroxy-methyl]-3-hydroxy-6-methyl-pyran-4(1H)-one (**2e**). The reaction was performed according to the general procedure using **1** (0.40 g, 3.2 mmol) and 3,4,5-trimethoxybenzaldehyde (0.68 g, 3.5 mmol, in 5 mL dioxane) affording a pale yellow solid (0.78 g, 69%). M.p. 182–184 °C; ¹H NMR (DMSO-*d*₆) δ: 2.22 (s, 3H, CH₃), 3.64 (s, 3H, 4'-OCH₃), 3.76 (s, 6H, 3'/5'-OCH₃), 5.95 (d, *J* = 5.2 Hz, 1H, CHOAr), 6.15 (d, *J* = 5.2 Hz, 1H, CHOAr), 6.20 (s, 1H, CH), 6.71 (s, 2H, Ar-H3'/H5'), 9.05 (brs, 1H, COH); ¹³C NMR (DMSO-*d*₆) δ: 19.7 (CH₃), 56.3 (3'/5'-OCH₃), 60.5 (4'-OCH₃) 66.4 (CHOAr), 103.7 (Ar-C2'/C6'), 111.6 (CH₃C=CH), 137.2 (Ar-C1'), 137.4 (Ar-C4'), 140.0 (CH₃C=CH), 150.8 (HOCHC=COH), 153.2 (Ar-C3'/C5'), 165.0 (CHOH), 174.3 (C=O); IR (KBr, cm⁻¹, selected bands): 3416, 3293, 1646, 1600, 1558, 1226, 1126; Elemental Anal. Calc. for C₁₆H₁₈O₇ · ¼H₂O: C, 58.80; H, 5.71. Found: C, 58.84; H, 5.42%.

4.2.2. General procedure for the synthesis of the Ru(II) complexes

The maltol-derived ligand (0.73 mmol) and sodium methoxide (43 mg, 0.80 mmol) were dissolved in methanol (15 mL) and stirred for 5 min under inert atmosphere to give a clear solution. Afterwards, bis[dichlorido(η⁶-*p*-cymene)ruthenium(II)] (200 mg, 0.33 mmol) was dissolved in CH₂Cl₂ (5 mL) and added dropwise to the reaction mixture which was stirred for further 5 (for **3a**) or 18 h. The reaction mixture was concentrated *in vacuo*, and the residue was extracted with CH₂Cl₂ (3 × 15 mL). The combined organic layers were filtered, and the solvent was removed. The crude product was purified by recrystallization or precipitation.

4.2.2.1. Chlorido[2-(hydroxy-phenyl-methyl)-6-methyl-3-(oxo-κO)-pyran-4(1H)-onato-κO4](η⁶-*p*-cymene)ruthenium(II) (**3a**). The reaction was performed according to the general complexation protocol using **2a** (168 mg, 0.73 mmol). The crude product was recrystallized from EtOAc/*n*-hexane affording a red crystalline solid (240 mg, 73%). M.p. 160–165 °C decomp.; MS (ESI⁺) *m/z* 391 [M–Cl]⁺; ¹H NMR (CDCl₃) δ: 1.30–1.38 (m, 6H, CH₃), 2.19 (s, 3H, CH₃,_{pyr}), 2.33 (s, 3H, CH₃,_{cym}), 2.93 (m, 1H, CH(CH₃)₂,_{cym}), 5.28–5.33 (m, 2H, Ar_{cym}-H3/H5), 5.52–5.57 (m, 2H, Ar_{cym}-H2/H6), 5.81 (s, 1H, CHOHPH), 5.86 (s, 1H, CHOHPH), 6.27 (s, 1H, CH), 7.30–7.50 (m, 5H, Ph); ¹³C NMR (CDCl₃) δ: 18.6 (CH₃), 19.8 (CH₃,_{cym}), 22.3 (CH₃,_{cym}), 31.2 (CH(CH₃)₂), 72.9 (CHOHPH), 78.2 (Ar_{cym}-C3/C5), 80.2 (Ar_{cym}-C2/C6), 95.8 (Ar_{cym}-C4), 99.5 (Ar_{cym}-C1), 109.4 (CH), 127.1 (Ph-C2), 128.0 (Ph), 128.5 (Ph), 141.5 (CH₃C=CH), 152.9 (Ph-C1), 155.1 (HOCHC=COH), 164.2 (CHOH), 185.0 (C=O); IR (KBr, cm⁻¹, selected bands): 3394, 1604, 1561, 1503, 1476, 1259, 1206; Elemental Anal. Calc. for C₂₃H₂₅ClO₄Ru: C, 55.03; H, 5.02. Found: C, 54.73; H, 5.02%.

4.2.2.2. Chlorido[2-(4-nitrophenyl)-hydroxy-methyl]-6-methyl-3-(oxo-κO)-pyran-4(1H)-onato-κO4](η⁶-*p*-cymene)ruthenium(II) (**3b**). The reaction was performed according to the general complexation protocol using **2b** (197 mg, 0.73 mmol). The crude product was recrystallized from EtOAc/diethyl ether/*n*-hexane

affording an orange powder (250 mg, 70%). M.p. 180–185 °C decomp.; MS (ESI⁺) *m/z* 512 [M–Cl]⁺; ¹H NMR (CDCl₃) δ: 1.31–1.40 (m, 6H, CH₃,_{cym}), 2.19 (s, 3H, CH₃,_{pyr}), 2.34 (s, 3H, CH₃,_{cym}), 2.92 (m, 1H, CH(CH₃)₂), 5.29–5.35 (m, 2H, Ar_{cym}-H3/H5); 5.51–5.58 (m, 2H, Ar_{cym}-H2/H6), 5.93 (bs, 1H, CHOAr), 5.99 (bs, 1H, CHOAr), 6.30 (s, 1H, CH), 7.67–7.70 (m, 2H, Ar_{cym}-H2/H6), 8.20–8.25 (m, 2H, Ar_{cym}-H3'/H5'); ¹³C NMR (CDCl₃) δ: 18.6 (CH₃,_{pyr}), 19.9 (CH₃,_{cym}), 22.5 (CH₃,_{cym}), 31.2 (CH(CH₃)₂), 71.7 (CHOAr), 78.0 (Ar_{cym}-C3/C5), 80.3 (Ar_{cym}-C2/C6), 95.7 (Ar_{cym}-C4), 99.4 (Ar_{cym}-C1), 109.5 (CH), 123.6 (Ar-C2/C6), 127.5 (Ar-C3/C5), 148.0 (Ar-C1), 148.6 (Ar-C4), 151.0 (CH₃C=CH), 155.5 (HOCHC=COH), 164.7 (CHOH), 185.2 (C=O); IR (KBr, cm⁻¹, selected bands): 3342, 1603, 1564, 1513, 1477, 1256, 1205; Elemental Anal. Calc. for C₂₃H₂₄ClNO₆Ru: C, 50.51; H, 4.42; N, 2.56. Found: C, 50.35; H, 4.39; N, 2.51%.

4.2.2.3. Chlorido[2-(4-fluorophenyl)-hydroxy-methyl]-6-methyl-3-(oxo-κO)-pyran-4(1H)-onato-κO4](η⁶-*p*-cymene)ruthenium(II) (**3c**). The reaction was performed according to the general complexation protocol using **2c** (183 mg, 0.73 mmol). The crude product was recrystallized from EtOAc/diethyl ether/*n*-hexane,

affording an orange powder (240 mg, 71%). M.p. 90–95 °C decomp.; MS (ESI⁺) *m/z* 485 [M–Cl]⁺; ¹H NMR (CDCl₃) δ: 1.30–1.38 (m, 6H, CH₃,_{cym}), 2.20 (s, 3H, CH₃,_{pyr}), 2.33 (s, 3H, CH₃,_{cym}), 2.92 (m, 1H, CH(CH₃)₂), 5.28–5.33 (m, 2H, Ar_{cym}-H3/H5), 5.53–5.57 (m, 2H, Ar_{cym}-H2/H6), 5.76 (bs, 1H, CHOAr), 5.89 (bs, 1H, CHOAr), 6.28 (s, 1H, CH), 6.99–7.07 (m, 2H, Ar-H3/H5), 7.46–7.48 (m, 2H, Ar-H2/H6); ¹³C NMR (CDCl₃) δ: 18.6 (CH₃,_{pyr}), 19.8 (CH₃,_{cym}), 22.4 (CH₃,_{cym}), 31.2 (CH(CH₃)₂), 72.2 (CHOAr), 78.1 (Ar_{cym}-C3/C5), 80.2 (Ar_{cym}-C2/C6), 95.7 (Ar_{cym}-C4), 99.3 (Ar_{cym}-C1), 109.4 (CH), 115.3 (*J* = 22.3 Hz, Ar-C3/C5), 128.5 (*J* = 8.0 Hz, Ar-C2/C6), 137.3 (*J* = 4.1 Hz, Ar-C1), 152.2 (CH₃C=CH), 155.2 (HOCHC=COH), 162.5 (*J* = 245.7 Hz, Ar-C4), 164.0 (CHOH), 185.0 (C=O); IR (KBr, cm⁻¹, selected bands): 3387, 1603, 1563, 1507, 1477, 1219; Elemental Anal. Calc. for C₂₃H₂₄ClFO₄Ru: C, 53.13; H, 4.65. Found: C, 52.86; H, 4.62%.

4.2.2.4. Chlorido[2-(3-fluorophenyl)-hydroxy-methyl]-6-methyl-3-(oxo-κO)-pyran-4(1H)-onato-κO4](η⁶-*p*-cymene)ruthenium(II) (**3d**). The reaction was performed according to the general complexation protocol using **2d** (183 mg, 0.73 mmol). The crude product was recrystallized from EtOAc/diethyl ether/*n*-hexane

affording an orange powder (250 mg, 73%). M.p. 160–165 °C decomp.; MS (ESI⁺) *m/z* 485 [M–Cl]⁺; ¹H NMR (CDCl₃) δ: 1.30–1.38 (m, 6H, CH₃,_{cym}), 2.20 (s, 3H, CH₃,_{pyr}), 2.33 (s, 3H, CH₃,_{cym}), 2.92 (m, 1H, CH(CH₃)₂), 5.30 (m, 2H, Ar_{cym}-H3/H5), 5.54 (m, 2H, Ar_{cym}-H2/H6), 5.83 (brs, 1H, CHOAr), 6.01 (brs, 1H, CHOAr), 6.28 (s, 1H, CH), 6.99 (m, 1H, Ar-H4), 7.22–7.33 (m, 3H, Ar-H2/H5/H6); ¹³C NMR (CDCl₃) δ: 18.6 (CH₃,_{pyr}), 19.8 (CH₃,_{cym}), 22.2 (CH₃,_{cym}), 31.2 (CH(CH₃)₂), 72.4 (CHOAr), 78.1 (Ar_{cym}-C3/C5), 80.2 (Ar_{cym}-C2/C6), 95.7 (Ar_{cym}-C4), 99.4 (Ar_{cym}-C1), 109.4 (CH), 113.9 (*J* = 22.3 Hz, Ar-C2), 114.7 (*J* = 22.2 Hz, Ar-C4), 122.3 (*J* = 3.0 Hz, Ar-C6), 129.9 (*J* = 7.4 Hz, Ar-C5), 144.0 (*J* = 7.2 Hz, Ar-C1), 152.1 (CH₃C=CH), 155.2 (HOCHC=COH), 162.8 (*J* = 262.4 Hz, Ar-C3), 164.2 (CHOH), 185.0 (C=O); IR (KBr, cm⁻¹, selected bands): 3396, 1604, 1562, 1504, 1476, 1250, 1203; Elemental Anal. Calc. for C₂₃H₂₄ClFO₄Ru: C, 53.13; H, 4.65. Found: C, 53.11; H, 4.65%.

4.2.2.5. Chlorido[2-(3,4,5-trimethoxyphenyl)-hydroxy-methyl]-6-methyl-3-(oxo-κO)-pyran-4(1H)-onato-κO4](η⁶-*p*-cymene)ruthenium(II) (**3e**). The reaction was performed according to the general complexation protocol using **2e** (234 mg, 0.73 mmol). The crude product was recrystallized from EtOAc/*n*-hexane, affording an orange powder (200 mg, 54%). M.p. 160–165 °C decomp.; MS (ESI⁺) *m/z* 557 [M–Cl]⁺; ¹H NMR (CDCl₃) δ: 1.37–1.39 (m, 6H, CH₃,_{cym}), 2.22 (s, 3H, CH₃,_{pyr}), 2.32 (s, 3H, CH₃,_{cym}), 2.93 (m, 1H, CH(CH₃)₂),

3.82 (s, 3H, 4'-OCH₃), 3.89 (s, 6H, 3'/5'-OCH₃) 5.29–5.31 (m, 2H, Ar_{cym}-H3/H5), 5.89 (m, 1H, CHOHar), 6.30 (s, 1H, CH), 6.72 (s, 2H, Ar-H2/H6); ¹³C NMR (CDCl₃) δ: 18.6 (CH₃,pyr), 19.8 (CH₃,cym), 22.3 (CH₃,cym), 31.2 (CH(CH₃)₂), 56.4 (3'/5'-OCH₃), 60.7 (4'-OCH₃), 71.8 (CHOHar), 77.8 (Ar_{cym}-C3/C5), 80.5 (Ar_{cym}-C2/C6), 95.4 (Ar_{cym}-C4), 99.0 (Ar_{cym}-C1), 104.3 (Ar-C2/C6), 109.4 (CH), 136.8 (Ar-C1), 137.8 (Ar-C4), 152.8 (CH₃C=CH), 153.3 (Ar-C3/C5), 155.2 (HOCHC=COH), 164.1 (CHOH), 185.0 (C=O); IR (KBr, cm⁻¹, selected bands): 3383, 1603, 1567, 1510, 1473, 1417, 1326, 1238, 1124; Elemental Anal. Calc. for C₂₆H₃₁ClO₇Ru: C, 52.75; H, 5.28. Found: C, 52.80; H, 5.32%.

4.3. GMP binding

Complexes **3a–e** (1–2 mg/mL) were dissolved in D₂O containing 5% DMSO-*d*₆. The solution was titrated with a 5'-GMP solution (10 mg/mL) in 50 μL increments, and the reaction was monitored by ¹H and ³¹P NMR spectroscopy until unreacted 5'-GMP was detected.

4.4. pK_a determination

Complexes **3a–e** were dissolved in D₂O containing 5% DMSO-*d*₆. The pH value was measured directly in the NMR tubes with an Eco Scan pH6 pH meter equipped with a glass-micro combination pH electrode (Orion 9826BN) and calibrated with standard buffer solutions of pH 4.00, 7.00 and 10.00. The pH titration was performed by addition of NaOD (0.4–0.0004% in D₂O) and DNO₃ (0.4–0.0004% in D₂O). The observed shifts of the Ar_{cym}-H2/H6 protons of the arene ring in the ¹H NMR spectra were plotted against the pH value, and the obtained curves were fitted using the Henderson-Hasselbalch equation with Excel software (Microsoft® Office Excel 2003, SP3, Microsoft Corporation). The experimentally obtained pK_a values were corrected with Eq. (1) [60], in order to convert the pK_a in D₂O to corresponding pK_a values in aqueous solutions.

$$pK_x = 0.929pK_{x^*} + 0.42 \quad (1)$$

4.5. Cytotoxicity in cancer cell lines

4.5.1. Cell lines and conditions

CH1 cells originate from an ascites sample of a patient with a papillary cystadenocarcinoma of the ovary and were a generous gift from Lloyd R. Kelland, CRC Centre for Cancer Therapeutics, Institute of Cancer Research, Sutton, UK. SW480 (adenocarcinoma of the colon) and A549 (non-small cell lung cancer) cells were kindly provided by Brigitte Marian (Institute of Cancer Research, Department of Medicine I, Medical University of Vienna, Austria). All cell culture reagents were obtained from Sigma–Aldrich Austria. Cells were grown in 75 cm² culture flasks (Iwaki) as adherent monolayer cultures in Minimal Essential Medium (MEM) supplemented with 10% heat-inactivated fetal calf serum, 1 mM sodium pyruvate, 4 mM L-glutamine and 1% non-essential amino acids (100×). Cultures were maintained at 37 °C in a humidified atmosphere containing 5% CO₂.

4.5.2. MTT assay conditions

Cytotoxicity was determined by the colorimetric MTT (3-(4,5-dimethyl-2-thiazolyl)-2,5-diphenyl-2H-tetrazolium bromide, purchased from Fluka) microculture assay. For this purpose, cells were harvested from culture flasks by trypsinization and seeded into 96-well microculture plates (Iwaki). Cell densities of 1.5 × 10³ cells/well (CH1), 2.5 × 10³ cells/well (SW480) and 4 × 10³ cells/well (A549) were chosen in order to ensure exponential growth throughout drug exposure. Cells were allowed to settle in drug-free complete culture medium for 24 h. Stocks of the test compounds in

DMSO were diluted in complete culture medium such that the maximum DMSO content did not exceed 1% (this procedure yielded opaque but colloidal solutions from which no precipitates could be separated by centrifugation). These dilutions were added in 200 μL aliquots to the microcultures after removal of the pre-incubation medium, and cells were exposed to the test compounds for 96 h. At the end of exposure, all media were replaced by 100 μL/well RPMI1640 culture medium (supplemented with 10% heat-inactivated fetal bovine serum and 4 mM L-glutamine) plus 20 μL/well MTT solution in phosphate-buffered saline (5 mg/mL). After incubation for 4 h, the supernatants were removed, and the formazan crystals formed by vital cells were dissolved in 150 μL DMSO per well. Optical densities at 550 nm were measured with a microplate reader (Tecan Spectra Classic), using a reference wavelength of 690 nm. The quantity of vital cells was expressed in terms of T/C values by comparison to untreated control microcultures, and 50% inhibitory concentrations (IC₅₀) were calculated from concentration–effect curves by interpolation. Evaluation is based on means from three independent experiments, each comprising six replicates per concentration level.

Acknowledgments

We thank the University of Vienna, the Hochschuljubiläumsstiftung Vienna (H1556-2006), the Theodor-Körner-Fonds, the Austrian Council for Research and Technology Development, the FFG – Austrian Research Promotion Agency (Project FA 526003), the FWF – Austrian Science Fund (Schrödinger Fellowship J2613-N19 [C.G.H.], project P18123-N11), the EPFL, and COST D39 for financial support. We gratefully acknowledge Alexander Roller for collecting and refining the X-ray diffraction data and Prof. Markus Galanski for recording the NMR spectra.

Appendix A. Supplementary material

CCDC 701753 contains the supplementary crystallographic data for **3b**. These data can be obtained free of charge from The Cambridge Crystallographic Data Centre via www.ccdc.cam.ac.uk/data_request/cif. Supplementary data associated with this article can be found, in the online version, at [doi:10.1016/j.jorgchem.2008.10.016](https://doi.org/10.1016/j.jorgchem.2008.10.016).

References

- [1] M.A. Jakupec, M. Galanski, V.B. Arion, C.G. Hartinger, B.K. Keppler, Dalton Trans. (2008) 183.
- [2] M.A. Jakupec, B.K. Keppler, Curr. Top. Med. Chem. 4 (2004) 1575.
- [3] W.H. Ang, P.J. Dyson, Eur. J. Inorg. Chem. (2006) 4003.
- [4] C.G. Hartinger, S. Zorbas-Seifried, M.A. Jakupec, B. Kynast, H. Zorbas, B.K. Keppler, J. Inorg. Biochem. 100 (2006) 891.
- [5] C.G. Hartinger, P.J. Dyson, Chem. Soc. Rev. (2008) doi:10.1039/B707077M.
- [6] U. Schatzschneider, N. Metzler-Nolte, Angew. Chem., Int. Ed. 45 (2006) 1504.
- [7] R. Alberto, Top. Curr. Chem. 252 (2005) 1.
- [8] J.M. Rademaker-Lakhai, D. van den Bongard, D. Pluim, J.H. Beijnen, J.H. Schellens, Clin. Cancer Res. 10 (2004) 3717.
- [9] C.G. Hartinger, M.A. Jakupec, S. Zorbas-Seifried, M. Groessl, A. Egger, W. Berger, H. Zorbas, P.J. Dyson, B.K. Keppler, Chem. Biodiversity 5 (2008) 2140.
- [10] M. Pongratz, P. Schluga, M.A. Jakupec, V.B. Arion, C.G. Hartinger, G. Allmaier, B.K. Keppler, J. Anal. At. Spectrom. 19 (2004) 46.
- [11] A.R. Timerbaev, A.V. Rudnev, O. Semenova, C.G. Hartinger, B.K. Keppler, Anal. Biochem. 341 (2005) 326.
- [12] M. Sulyok, S. Hann, C.G. Hartinger, B.K. Keppler, G. Stinger, G. Koellensperger, J. Anal. At. Spectrom. 20 (2005) 856.
- [13] C.G. Hartinger, S. Hann, G. Koellensperger, M. Sulyok, M. Grössl, A.R. Timerbaev, A.V. Rudnev, G. Stinger, B.K. Keppler, Int. J. Clin. Pharmacol. Ther. 43 (2005) 583.
- [14] A.R. Timerbaev, C.G. Hartinger, S.S. Aleksenko, B.K. Keppler, Chem. Rev. 106 (2006) 2224.
- [15] K. Polec-Pawlak, J.K. Abramski, O. Semenova, C.G. Hartinger, A.R. Timerbaev, B.K. Keppler, M. Jarosz, Electrophoresis 27 (2006) 1128.
- [16] P. Schluga, C.G. Hartinger, A. Egger, E. Reisner, M. Galanski, M.A. Jakupec, B.K. Keppler, Dalton Trans. (2006) 1796.

- [17] A. Vessieres, S. Top, W. Beck, E. Hillard, G. Jaouen, Dalton Trans. (2006) 529.
- [18] K. Strohfeldt, M. Tacke, Chem. Soc. Rev. 37 (2008) 1174.
- [19] A. Casini, C. Hartinger, C. Gabbiani, E. Mini, P.J. Dyson, B.K. Keppler, L. Messori, J. Inorg. Biochem. 102 (2008) 564.
- [20] C.S. Allardyce, P.J. Dyson, D.J. Ellis, S.L. Heath, Chem. Commun. (2001) 1396.
- [21] C. Sclaro, A. Bergamo, L. Brescacin, R. Delfino, M. Cocchietto, G. Laurenczy, T.J. Geldbach, G. Sava, P.J. Dyson, J. Med. Chem. 48 (2005) 4161.
- [22] Y.K. Yan, M. Melchart, A. Habtemariam, P.J. Sadler, Chem. Commun. (2005) 4764.
- [23] W.H. Ang, E. Daldini, C. Sclaro, R. Scopelliti, L. Juillerat-Jeanerret, P.J. Dyson, Inorg. Chem. 45 (2006) 9006.
- [24] C. Sclaro, T.J. Geldbach, S. Rochat, A. Dorcier, C. Gossens, A. Bergamo, M. Cocchietto, I. Tavernelli, G. Sava, U. Rothlisberger, P.J. Dyson, Organometallics 25 (2006) 756.
- [25] J.É. Debreczeni, A.N. Bullock, G.E. Atilla, D.S. Williams, H. Bregman, S. Knapp, E. Meggers, Angew. Chem. 45 (2006) 1580.
- [26] C. Sclaro, A.B. Chaplin, C.G. Hartinger, A. Bergamo, M. Cocchietto, B.K. Keppler, G. Sava, P.J. Dyson, Dalton Trans. (2007) 5065.
- [27] C.A. Vock, W.H. Ang, C. Sclaro, A.D. Phillips, L. Lagopoulos, L. Juillerat-Jeanerret, G. Sava, R. Scopelliti, P.J. Dyson, J. Med. Chem. 50 (2007) 2166.
- [28] A.F.A. Peacock, M. Melchart, R.J. Deeth, A. Habtemariam, S. Parsons, P.J. Sadler, Chem. Eur. J. 13 (2007) 2601.
- [29] W.F. Schmid, R.O. John, V.B. Arion, M.A. Jakupec, B.K. Keppler, Organometallics 26 (2007) 6643.
- [30] W.F. Schmid, R.O. John, G. Mühlgassner, P. Heffeter, M.A. Jakupec, M. Galanski, W. Berger, V.B. Arion, B.K. Keppler, J. Med. Chem. 50 (2007) 6343.
- [31] M.G. Mendoza-Ferri, C.G. Hartinger, R.E. Eichinger, N. Stolyarova, K. Severin, M.A. Jakupec, A.A. Nazarov, B.K. Keppler, Organometallics 27 (2008) 2405.
- [32] M.G. Mendoza-Ferri, C.G. Hartinger, A.A. Nazarov, W. Kandioller, K. Severin, B.K. Keppler, Appl. Organomet. Chem. 22 (2008) 326.
- [33] W.H. Ang, A. De Luca, C. Chapuis-Bernasconi, L. Juillerat-Jeanerret, M. Lo Bello, P.J. Dyson, ChemMedChem 2 (2007) 1799.
- [34] F. Schmitt, P. Govindaswamy, G. Suess-Fink, W.H. Ang, P.J. Dyson, L. Juillerat-Jeanerret, B. Therrien, J. Med. Chem. 51 (2008) 1811.
- [35] W.H. Ang, E. Daldini, L. Juillerat-Jeanerret, P.J. Dyson, Inorg. Chem. 46 (2007) 9048.
- [36] P.J. Dyson, G. Sava, Dalton Trans. (2006) 1929.
- [37] S. Chatterjee, S. Kundu, A. Bhattacharyya, C.G. Hartinger, P.J. Dyson, J. Biol. Inorg. Chem. 13 (2008) 1149.
- [38] O. Nováková, A.A. Nazarov, C.G. Hartinger, B.K. Keppler, V. Brabec, Biochem. Pharmacol., in press, doi:10.1016/j.bcp.2008.10.021.
- [39] K.H. Thompson, C. Orvig, Dalton Trans. (2006) 761.
- [40] K. Saatchi, K.H. Thompson, B.O. Patrick, M. Pink, V.G. Yuen, J.H. McNeill, C. Orvig, Inorg. Chem. 44 (2005) 2689.
- [41] K.H. Thompson, C.A. Barta, C. Orvig, Chem. Soc. Rev. 35 (2006) 545.
- [42] Z.-S. Lu, J. Burgess, R. Lane, Transition Met. Chem. 27 (2002) 239.
- [43] D.T. Puerta, M. Botta, C.J. Jocher, E.J. Werner, S. Avedano, K.N. Raymond, S.M. Cohen, J. Am. Chem. Soc. 128 (2006) 2222.
- [44] C.-T. Yang, S.G. Sreerama, W.-Y. Hsieh, S. Liu, Inorg. Chem. 47 (2008) 2719.
- [45] M. Backlund, J. Ziller, P.J. Farmer, Inorg. Chem. 47 (2008) 2864.
- [46] Y. Ma, W. Luo, P.J. Quinn, Z. Liu, R.C. Hider, J. Med. Chem. 47 (2004) 6349.
- [47] A.P. Abbott, G. Capper, D.L. Davies, J. Fawcett, D.R. Russell, J. Chem. Soc., Dalton Trans. (1995) 3709.
- [48] R. Lang, K. Polborn, T. Severin, K. Severin, Inorg. Chim. Acta 294 (1999) 62.
- [49] M.D. Aytémir, U. Calis, M. Ozalp, Arch. Pharm. (Weinheim, Ger.), 337 (2004) 281.
- [50] W.-Y. Hsieh, C.M. Zaleski, V.L. Pecoraro, P.E. Fanwick, S. Liu, Inorg. Chim. Acta 359 (2006) 228.
- [51] J.L. Lamboy, A. Pasquale, A.L. Rheingold, E. Melendez, Inorg. Chim. Acta 360 (2007) 2115.
- [52] U. Warnke, C. Rappel, H. Meier, C. Kloft, M. Galanski, C.G. Hartinger, B.K. Keppler, U. Jaehde, ChemBioChem 5 (2004) 1543.
- [53] A. Dorcier, C.G. Hartinger, R. Scopelliti, R.H. Fish, B.K. Keppler, P.J. Dyson, J. Inorg. Biochem. 102 (2008) 1066.
- [54] M.A. Bennett, T.N. Huang, T.W. Matheson, A.K. Smith, Inorg. Synth. 21 (1982) 74.
- [55] M.R. Pressprich, J. Chambers, SAINT + Integration Engine, Program for Crystal Structure Integration, Madison, 2004.
- [56] G.M. Sheldrick, SHELXS-97, Program for Crystal Structure Solution, University Göttingen, Germany, 1997.
- [57] G.M. Sheldrick, SHELXL-97, Program for Crystal Structure Refinement, University Göttingen, Germany, 1997.
- [58] L.J. Farrugia, J. Appl. Crystallogr. 30 (1997) 565.
- [59] International Tables for X-ray Crystallography, Kluwer Academic Press, Dordrecht, The Netherlands, 1992.
- [60] A. Krezel, W. Bal, J. Inorg. Biochem. 98 (2004) 161.